Effective Hamiltonian for the impurity-impurity interaction in micropillars in the presence of decoherence

J. A. Andrade and A. A. Aligia
Centro Atómico Bariloche and Instituto Balseiro, Comisión Nacional de Energía Atómica, 8400 Bariloche, Argentina

G. F. Quinteiro
Departamento de Física and IFIBA, FCEyN, Universidad de Buenos Aires, Pabellón 1, Ciudad Universitaria, 1428 Buenos Aires, Argentina

(Received 9 December 2011; revised manuscript received 25 January 2012; published 11 April 2012)

We study the optically induced effective interaction between spins in micropillars. Our theoretical model describes a circularly polarized cavity mode strongly coupled to two quantum-dot excitons, each of which interacts with a localized spin. The decoherence effect inducing a finite lifetime to the cavity mode is included. Using the master equation for the density matrix we investigate the dynamics under low-power excitation. In the absence of decoherence, we recover the result obtained in a previous work (which uses conventional low-energy reduction procedures) for an effective Hamiltonian containing a Zeeman term and an Ising interaction between the localized spins. For finite cavity-photon lifetime we employ Fourier analysis on the time dependence of the nondiagonal element of the reduced density matrix, obtained by tracing out the photons and excitons, to find a quasieffective spin-spin Ising Hamiltonian. This Hamiltonian is a possible building block for two-qubit quantum computing operation. We study how decoherence affects the construction of that effective interaction. Finally, we discuss the possible application for transition-metal impurity spins embedded in CdTe quantum dots.

DOI: 10.1103/PhysRevB.85.165421 PACS number(s): 78.67.−n, 71.36.+c, 73.21.La, 03.65.Yz

I. INTRODUCTION

Hybrid (matter-photon) systems hold great promise for the development of quantum communication and computing, exploiting quantum states of spins or quantum dots (QDs) for local storage and processing, and the long-distance transmission of the photons.[1–5] It has been demonstrated that the state of a Mn spin in a CdTe QD can be manipulated by suitable optical-induced exciton transitions,[6–8] and the effective light Mn interaction can be engineered using quantum interference effects.[9] Very recently, optical pumping and nondestructive readout of a single ± 1 spin an InAs/GaAs has been demonstrated.[10] In this system, the effective spin is an acceptor state of the Mn atom. The dynamics of the impurity spins can be followed by time-resolved Kerr rotation.[11] An interesting aspect of the photoluminescence decay of the excitons (bound states of an electron and a hole) and trions (bound states of two electrons and a hole)[12,13] and the creation of an exciton[14] is the manifestation of the hybridization of the spin localized in the QD with a continuum of extended states, and the related Kondo effect.

When the coupling between excitons and photons is strong compared to their decay rates times $\hbar$, the system is in the strong coupling (SC) regime. The SC between single (In,Ga)As QDs and micropillar cavity modes[15] has become apparent in photoluminescence data which displayed anticrossings between the QD exciton and cavity-mode dispersion relations.[7,15,16] The luminescence spectra of QDs in microcavities has been calculated taking into account dissipation effects using master equations.[17,18] The SC regime is also displayed in resonant Raman scattering due to optical phonons in planar II-VI-type semiconductor microcavities.[19,20] Recent advances include studies in the deep strong-coupling regime[21,22] and the exact solution of the Rabi model.[23]

Imamoglu *et al.*[2] showed the possibility of inducing an effective interaction between spins in QDs mediated by photons. This interaction permits us to perform two-qubit operations, essential for quantum computing. Later, the optically induced interaction between $1/2$ spins in a two-dimensional (2D) microcavity[4] and in a zero-dimensional one[24] has been calculated. Due to selection rules, the light mediated effective spin-spin interaction is of the Ising type ($I S_1^z S_2^z$).[24] It has been shown that this interaction is sufficient to perform two-qubit operations.[25]

Recently, we have solved the energy spectrum of a model that describes a circularly polarized cavity mode strongly coupled to two exciton modes, each of which interacts with a localized spin of arbitrary magnitude.[26] In the SC regime, the low-energy part of the spectrum can be described by an effective spin model, which contains a magnetic field, an axial anisotropy, and an Ising interaction between the localized spins. Since decoherence effects were absent, the derivation of the low-energy effective Hamiltonian at low temperatures has been done mapping the low-energy spectrum, a method widely known and used, for example, in cuprates and other transition-metal compounds.[27–34] At high temperatures, the effective Hamiltonian was constructed in such a way that it leads to the same reduced density matrix $\rho_{\rm eff}$, obtained tracing the excitonic and photonic degrees of freedom.[26]

The goal of this work is to obtain the parameters of the effective Hamiltonian and to study the dynamics of the system in the presence of decoherence caused by the leaking of the cavity mode, which decays into radiative modes. We have not included the decay of the excitons and impurity spins because they are smaller in present experimental setups. Extension of the method to include this effect is straightforward. Since the standard methods mentioned above to obtain effective Hamiltonians do not work in the presence of decoherence, we have determined the effective parameters from the evolution of the nondiagonal terms of $\rho_{\rm eff}$, starting from initial states suitably prepared. The time evolution of the full density matrix

$\rho(t)$ is obtained solving a master equation that includes the effects of decoherence.[35] For an infinite lifetime of the cavity photon, the results coincide with those obtained previously,[26] while for short lifetimes, the method to derive the effective parameters [from peaks in the Fourier transform of $\rho_{\rm eff}(t)$] fails due do lack of definition of any peaks in the nondiagonal term of $\rho_{\rm eff}(\omega)$. However, for intermediate values of the lifetime, our method yields the desired parameters, together with an estimate of the uncertainties. Moreover, for short lifetimes, for which our method fails, the system is not useful for quantum computation.

In Sec. II we present the model and method. In Sec. III the results for the determination of the parameters of the effective model are presented. In Sec. IV we analyze possible applications of the system to quantum computing. Section V contains a summary and a discussion.

II. MODEL AND METHODS

The model describes a cavity photon mode, interacting with the excitonic degrees of freedom of two QDs (represented by spins 1/2). In addition, the electron and hole of each exciton have a spin exchange interaction with a localized spin, and the photon mode interacts with a continuum of radiative modes. A scheme of the system is shown in Fig. 1.

From the above considerations, the Hamiltonian takes the form

$$\begin{aligned} H_r &= H + \sum_k \epsilon_k b_k^\dagger b_k + \sum_k (V_k a^\dagger b_k + \text{H.c.}), \\ H &= E_c a^\dagger a + \sum_{i=1}^{2} \left[E_x \sigma_i^z + g(\sigma_i^- a^\dagger + \text{H.c.}) \right. \\ &\quad \left. + J\left(\sigma_i^z + 1/2\right) S_i^z \right], \end{aligned} \tag{1}$$

where $a^\dagger$ is the creation operator of the cavity mode, σ_i^z, σ_i^+, and σ_i^- are spin operators for the two-level system of QD i, with ground ($|i\downarrow\rangle$) and excited ($|i\uparrow\rangle$) states which represent zero and one exciton, respectively, S_i^z is the spin projection of the localized spin i, and b_k is the destruction operator mode k inside a continuum of radiative modes. The first three terms

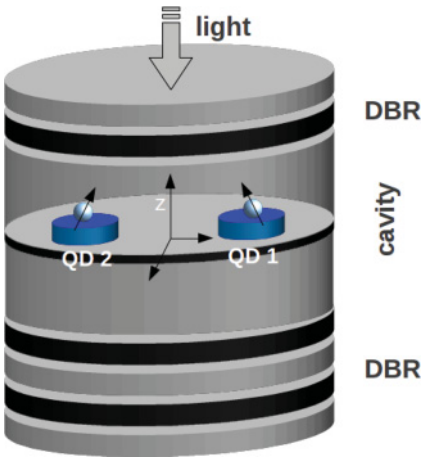

FIG. 1. (Color online) Scheme of the system: a 0D cavity encloses two QDs, each coupled to a single impurity spin of arbitrary magnitude.

of H are a generalization of the Jaynes-Cummings model[35] to two excitonic degrees of freedom. A similar model was used to study entanglement and bistability in coupled quantum dots inside a driven cavity.[36] The fourth one contains the Ising interaction between the excitons and the spins. The reason that only Ising interactions are present is the following. The symmetry of the cavity splits heavy holes (HHs) with angular momentum projection $j_z = \pm 3/2$ from the light holes (LHs) with $j_z = \pm 1/2$, which lie at higher energy. We assume that the light is circularly polarized with spin projection $j_z = 1$. Thus there is only one low-lying possible bright exciton which can be excited by this light, and corresponds to $j_z = -1/2$ (3/2) for the electron (HH) (the polarization subscripts are trivial and were dropped). The dark excitons with total angular momentum projection $j_z = \pm 2$ do not mix with the light and can be disregarded at low enough temperature. The spin-spin interaction between excitons and localized spins includes two types of exchange interactions, the anisotropic (Ising) one between the heavy hole and the localized spin, and the isotropic (Heisenberg) one between the electron and the localized spin.[37] The spin-flip terms lead to a mixing of the bright excitons with others (dark or containing LHs) lying at higher energies and can be neglected. It is interesting to note that the interaction J in CdTe QDs can be controlled using quantum interference effects.[9]

In this work we consider only two spin projections for Mn, namely $J_z = \pm 5/2$, since they are enough for quantum computing, and specific transitions can be controlled.[38] In III-V QDs, however, the Mn impurities form acceptor states with effective spin $J_z = \pm 1$.[10] Our model is of course directly applicable to this case with obvious changes.

The last term of H_r in Eq. (1) is responsible for a finite decay time of the cavity mode. Under general assumptions (see Chap. 15 of Ref. 35), the effect of this term can be incorporated in the form of a finite lifetime τ in the master equation that describes the evolution of the density matrix ρ of the system:

$$\frac{d\rho}{dt} = -\frac{i}{\hbar}[H,\rho] + \frac{1}{2\tau}(2a\rho a^\dagger - a^\dagger a\rho - \rho a^\dagger a), \tag{2}$$

where

$$\frac{1}{\tau} = 2\pi d(E_c)|V_k(E_c)|^2, \tag{3}$$

$d(E)$ is the density of the modes b_k at the energy E, and $|V_k(E)|^2$ is the average strength of the hybridization at the same energy. However, τ might be considered as a phenomenological parameter which includes other sources of decoherence as well.

We solve the set of differential equations (2) using Taylor's expansion in ρ up to second order. In the numerical calculation, it takes the form

$$\rho_{i+1} = \rho_i + \frac{d\rho_i}{dt}\Delta t + \frac{1}{2}\frac{d^2\rho_i}{dt^2}\Delta t^2, \tag{4}$$

where $d\rho_i/dt$ is taken from Eq. (2) and $d^2\rho_i/dt^2$ is obtained differentiating the second member of Eq. (2). Here i is the time index and Δt is the step, which in the present study is taken as $\Delta t = 0.05$ ps. For each time, we calculate the effective spin-density matrix taking the partial trace Tr_x over exciton

and photon variables,

$$\rho_{\rm eff}(t) = {\rm Tr}_x \rho(t), \tag{5}$$

and the Fourier transform of the nondiagonal matrix element of $\rho_{\rm eff}(t)$ was calculated by the routine "four1" of "Numerical Recipes in C."[39] The total time to make the numerical Fourier transform was 100 ns, and no difference in the results was observed by taking a smaller Δt.

As we have discussed before in absence of decoherence ($\tau \to \infty$),[26] one can restrict the Mn states to $S_i^z = \pm 5/2$, and the low-energy effective Hamiltonian for the spin dynamics takes the form (except for a constant)

$$H_{\rm eff} = B(S_1^z + S_2^z) + I S_1^z S_2^z, \tag{6}$$

where B and I are effective parameters, and the spin-density matrix at zero temperature $\rho_{\rm eff}^0$ becomes very simple in terms of eigenstates $|l\rangle$ and the corresponding eigenvalues E_l of $H_{\rm eff}$. In particular $\langle k|\rho_{\rm eff}^0(t)|l\rangle = \langle k|\rho_{\rm eff}^0(0)|l\rangle \exp[-i\omega_{kl}t]$, with $\omega_{kl} = (E_k - E_l)/\hbar$. Then, if for example, at time $t = 0$, a state $(|\alpha\rangle + |\beta\rangle)/\sqrt{2}$ is prepared, where $|\alpha\rangle = |\uparrow\uparrow\rangle$ ($S_1^z = S_2^z = 5/2$), and $|\beta\rangle = |\uparrow\downarrow\rangle$ ($S_1^z = 5/2$, $S_2^z = -5/2$), the Fourier transform of $\langle\beta|\rho_{\rm eff}^0(t)|\alpha\rangle$ (defined as $\int \langle\beta|\rho_{\rm eff}^0(t)|\alpha\rangle \exp(i\omega t)dt$) yields a linear combination of δ functions $\delta(\omega_{\beta\alpha} - \omega)$, and thus the difference $E_\alpha - E_\beta = 5B + 25I/2$ can be extracted from the position of the corresponding peak. Repeating the procedure with the state $|\alpha\rangle$ replaced by $|\downarrow\downarrow\rangle$, the result changes to $-5B + 25I/2$. Then, the Fourier transform of two experiments like these allows us to obtain the parameters B and I.

In the presence of decoherence, we repeat this procedure and calculate the Fourier transform of $\rho_{\rm eff}(t)$, starting from two spin states, linear combinations of two different eigenstates of $H_{\rm eff}$, and a given occupation of photons and excitons as described below. It is also possible to select a single time evolution at the cost of losing accuracy (see Sec. V). Now, instead of δ functions, the spectrum has several broad peaks, and many of them correspond to high-energy excitations which are not of interest. In any case, from the whole spectrum in the absence of decoherence, we can identify the peak of interest and (unless τ is too short, as discussed below) calculate B and I with an error which depends on the magnitude of the decoherence time τ.

Without loss of generality we assume $g > 0$ (the phase of $a^\dagger$ can be changed), and we define the detuning as the difference between cavity and exciton energies $\delta = E_c - E_x$.

III. RESULTS

In this section we apply the method described above to particular situations. Two different cases are considered, according to the initial state of the system dynamics having (i) one photon, (ii) one exciton. For each case, two different spin configurations of the initial state are considered. We have used the following parameters: $\delta = 1$ meV, $g = 0.5$ meV, and $J = 0.1$ meV.

A. Initial state with one cavity photon

In this subsection, we start at time $t = 0$ from a state with one cavity photon and no excitons ($|100\rangle$ where the numbers inside the ket denote the occupation of the cavity photon, exciton 1, and exciton 2, respectively) and two possible spin-wave functions: (i) $(|\downarrow\downarrow\rangle + |\uparrow\downarrow\rangle)/\sqrt{2}$, and (ii) $(|\downarrow\downarrow\rangle + |\uparrow\uparrow\rangle)/\sqrt{2}$.

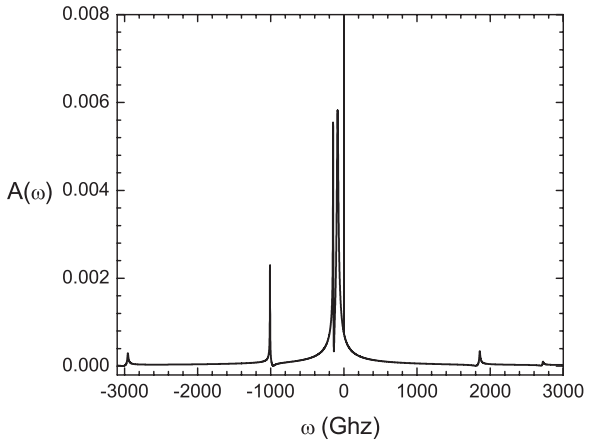

FIG. 2. Fourier amplitude of matrix element $\langle\downarrow\downarrow|\rho_{\rm eff}(t)|\uparrow\downarrow\rangle$ with photonic initial state and coherence time of 500 ps.

In case (i), starting from the state $|100\rangle(|\downarrow\downarrow\rangle + |\uparrow\downarrow\rangle)/\sqrt{2}$, we have let the system evolve during 100 ns, and the Fourier transform of matrix element $A(t) = \langle\downarrow\downarrow|\rho_{\rm eff}(t)|\uparrow\downarrow\rangle$ defined as $A(\omega) \propto \int A(t)\exp[i\omega t]dt$ was calculated. We have normalized the Fourier component in such a way that $\int A(\omega)d\omega = 1$. In Fig. 2 we show the Fourier amplitude for $\tau = 500$ ns. One can see several peaks, the frequencies of which correspond approximately to differences between eigenenergies of the Hamiltonian H, Eq. (1). The broadening and shift of the peaks are due to the effect of decoherence. H conserves S_1^z and S_2^z and has three eigenvalues for each value of S_1^z and S_2^z. The solution of H was discussed in a previous publication.[26] Because of symmetry, the state $|100\rangle|\downarrow\downarrow\rangle$ has overlap only to the lowest ($|1\rangle$) and highest ($|3\rangle$) eigenstates in the sector of $S_1^z = S_2^z = -5/2$. Instead, the state $|100\rangle|\uparrow\downarrow\rangle$ has a nonvanishing overlap with the three eigenstates ($|j'\rangle$) of H in the sector of $S_1^z = 5/2$, $S_2^z = -5/2$. Then, for $\tau \to \infty$, one has six δ function peaks at frequencies $\omega_{ij'} = (E_i - E_{j'})/\hbar$. They are $\omega_{11'} = -147$ Ghz, $\omega_{12'} = -1010.3$ Ghz, $\omega_{13'} = -2954.4$ Ghz, $\omega_{31'} = 2720.6$ Ghz, $\omega_{32'} = 1857.3$ Ghz, and $\omega_{33'} = -86.7$ Ghz. We are interested only in the first peak, which gives information on the effective Hamiltonian [Eq. (6)], as described in the previous section. In addition, there is a peak at $\omega = 0$, which is entirely due to decoherence, because it introduces states with no particles (excitons or photons). Note that in the absence of particles and an external magnetic field, the energy of the different spin states is zero and then leaking of the photons gives rise to contributions to $\rho_{\rm eff}(\omega)$ at frequency $\omega_{ii'} = 0$ [like Eq. (7)].

In Fig. 3 we show an expansion of the previous figure for small frequency, and we add also the corresponding information for two other decoherence times. As expected, the peaks broaden as τ decreases, although still for $\tau = 50$ ns, a broad peak near the frequency $\omega_{11'}$ of the ideal case $\tau \to \infty$ is still present. From the two points at which this peak reaches half of its maximum value, we can estimate the transition energy $\Delta E = \hbar\omega_{11'}$ from $|\downarrow\downarrow\rangle$ to $|\uparrow\downarrow\rangle$ of $H_{\rm eff}$ in the presence of decoherence. We obtain $\Delta E = -97 \pm 3$ μeV for

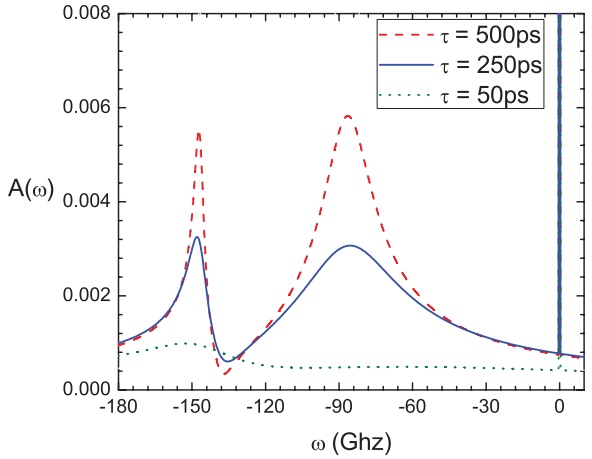

FIG. 3. (Color online) Fourier amplitude of matrix element $\langle\downarrow\downarrow|\rho_{\rm eff}(t)|\uparrow\downarrow\rangle$ for small frequency with photonic initial state and different coherence times.

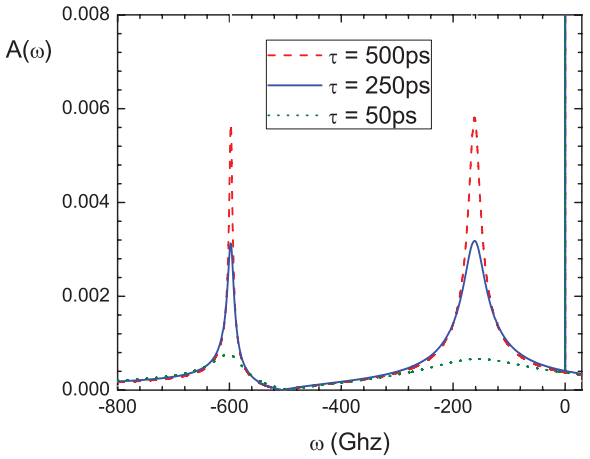

FIG. 5. (Color online) Fourier amplitude of matrix element $\langle\downarrow\downarrow|\rho_{\rm eff}(t)|\uparrow\uparrow\rangle$ for small frequency with photonic initial state and and different coherence times.

$\tau = 500$ ns, $\Delta E = -97 \pm 6$ μeV for $\tau = 250$ ns, and $\Delta E = -100 \pm 35$ μeV for $\tau = 50$ ns. This energy corresponds to $\Delta E = -5B + 25I/2$ in $H_{\rm eff}$ [see Eq. (6)].

To gain insight into the effects of decoherence, we plot in Fig. 4 the evolution of $\mathrm{Tr}\rho^2$ as a function of time. This quantity is 1 for a pure state, and since we have started from such a state (and a pure quantum evolution in a closed system conserves $\mathrm{Tr}\rho^2$), a deviation from 1 is a measure of the effects of decoherence. One sees a first decay of $\mathrm{Tr}\rho^2$ with a characteristic time of the order of τ. For longer times, as the photon leaks away, some states disappear in the quantum mixture and $\mathrm{Tr}\rho^2$ increases again. For the largest decoherence times τ of Fig. 2, the density matrix at long times has approximately the form

$$\rho \simeq \tfrac{1}{2}|000\rangle\langle 000|(|\downarrow\downarrow\rangle\langle\downarrow\downarrow| + |\uparrow\downarrow\rangle\langle\uparrow\downarrow|), \qquad (7)$$

which explains why $\mathrm{Tr}\rho^2 \simeq 1/2$ at long times. Instead for the smallest τ the photon decays fast before a large decoherence in the spin system takes place and therefore a large portion of the pure state $|000\rangle(|\downarrow\downarrow\rangle + |\uparrow\downarrow\rangle)/\sqrt{2}$ is present in the system at long times.

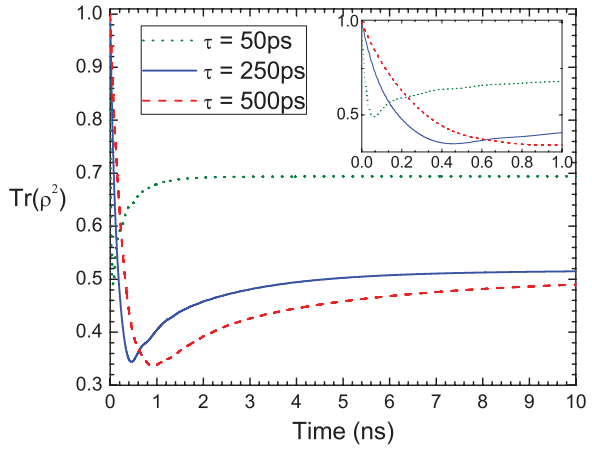

FIG. 4. (Color online) Trace of ρ^2 as a function of time with photonic initial state and different coherence times.

We have repeated the procedure in case (ii), for an initial state $|100\rangle(|\downarrow\downarrow\rangle + |\uparrow\uparrow\rangle)/\sqrt{2}$. The low-frequency spectra of matrix element $\langle\downarrow\downarrow|\rho_{\rm eff}(t)|\uparrow\uparrow\rangle$ are shown in Fig. 5.

The resulting numerical values of the corresponding excitation energy are $\Delta\tilde{E} = -394 \pm 3$ μeV for $\tau = 500$ ns, $\Delta\tilde{E} = -394 \pm 6$ μeV for $\tau = 250$ ns, and $\Delta\tilde{E} = -397 \pm 35$ μeV for $\tau = 50$ ns. According to $H_{\rm eff}$ [see Eq. (6)], $\Delta\tilde{E} = -10B$. Combining with the previous results for the energy difference in case (i), we can obtain $B = -\Delta\tilde{E}/10$ and $I = (2\Delta E - \Delta\tilde{E})/25$. The resulting values of the interaction are showed in Table I. Note that there is no significant change in I as the decoherence increases.

B. Initial state with one exciton

We have repeated the procedure above starting from an initial state with only one exciton excited. Specifically, we performed two calculations for an initial state (i) $|010\rangle(|\downarrow\downarrow\rangle + |\uparrow\downarrow\rangle)/\sqrt{2}$, and (ii) $|010\rangle(|\downarrow\downarrow\rangle + |\uparrow\uparrow\rangle)/\sqrt{2}$. In Fig. 6 we show the resulting low-energy part of the spectrum $A(\omega)$ for the first case. The peaks are approximately at the same position as before (compare with Fig. 3), but the intensity is different due to the different overlap of the (evolving) state of the system with the eigenstates of H. The relevant peak near $\omega_{11'} = -147$ Ghz is more intense and better resolved.

The low-energy part of the spectrum in case (ii) is displayed in Fig. 7. Comparison with Fig. 5 again shows that when the initial state has excitonic character, the peaks of $A(\omega)$ are better resolved. This results in values of the effective interaction I with smaller errors. The resulting values of the interaction are

TABLE I. Spin-spin effective interaction with its error for different lifetimes and with photonic initial state.

I (μeV)	Error (μeV)	τ (ps)
8	± 3.1	50
8	± 0.5	250
8	± 0.2	500

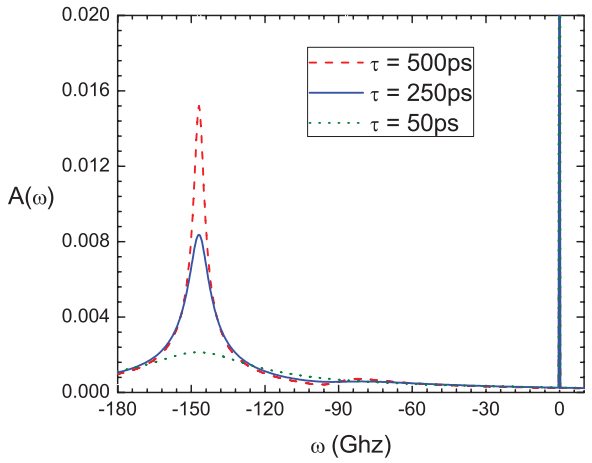

FIG. 6. (Color online) Fourier amplitude of matrix element $\langle\downarrow\downarrow|\rho_{\text{eff}}(t)|\uparrow\downarrow\rangle$ for small frequency with excitonic initial state and different coherence times.

shown in Table II. Note that there is not a significant change in I as the decoherence increases.

In contrast to the case with photonic initial state (see Figs. 2 and 5), $A(\omega)$ displayed in Fig. 7 contains an extra peak (very narrow and high) at -759.64 Ghz. This peak is due to a transition between antisymmetric eigenstates of H, which do not mix with states containing a photon, and therefore they are not affected by decoherence. The half width at half maximum of the peak in the figure (0.3 ns) is entirely due to the finite time (100 ns) used in the Fourier transform. In addition, the results are less affected by decoherence due to the fact that they only included photonic decay. Therefore, when no photons are present in the initial state, a photon should be created by the dynamics of the system before any decoherence process becomes possible. This is apparent also in the evolution of $\text{Tr}\rho^2$ when the initial state is $|010\rangle(|\downarrow\downarrow\rangle + |\uparrow\downarrow\rangle)/\sqrt{2}$, displayed in Fig. 8. The decay times are longer than in the previous case (compare with Fig. 4).

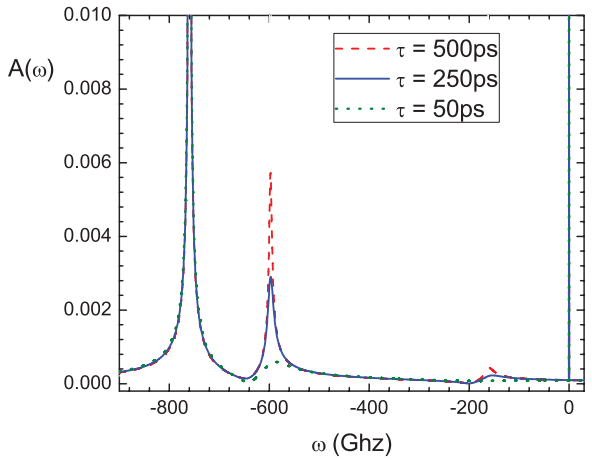

FIG. 7. (Color online) Fourier amplitude of matrix element $\langle\downarrow\downarrow|\rho_{\text{eff}}(t)|\uparrow\uparrow\rangle$ for small frequency with excitonic initial state and different coherence times.

TABLE II. Spin-spin effective interaction spin-spin with its error for different lifetimes and with excitonic initial state.

I (μeV)	Error (μeV)	τ (ps)
8	± 2.4	50
8	± 0.4	250
8	± 0.2	500

IV. APPLICATIONS

Micropillar cavities based on II-VI materials are promising systems for technological applications, for the elevated temperatures at which they can operate and the strong light-exciton coupling which they may have.[40] Naturally suited to these system are magnetic impurities like Mn^{2+} or Co^{2+}, which have spin 5/2 and 3/2, respectively. Among the II-VI materials, CdTe has been extensively studied, and important progress in the fabrication of micropillar systems embedding QDs and Mn impurities has been achieved.

Hereafter we apply our model to the particular case of two CdTe/ZnTe QDs, each one containing (or having in its vicinity) a single Mn ($S = 5/2$) magnetic impurity, all embedded in a II-VI semiconductor-based micropillar. These micropillar structures, of a diameter of a few micrometers, can be made to embed CdTe/ZnTe QDs and exhibit large Q factors.[41] Due to their size, the separation between different photon modes is large enough to consider them as single-mode systems, for example, a micropillar of height $h = 0.1$ μm and diameter $\phi = 2$ μm has energy levels separated by about $E = 10$ meV, larger than any energy of the system.

We focus on applications to quantum computing. Optically excited solid-state systems are considered as possible candidates for quantum computing, because they promise easy scalability, e.g., micropillars contain usually hundreds of QDs.[42] However, the main drawback is the large number of degrees of freedom interacting with the system, and thus the study of decoherence that may degrade the operation, and possible control of it, is a must. Systems such as the one considered in this work present different decay channels: exciton recombination, excitonic-spin decoherence, photon leakage, and Mn-spin decoherence. In the case of excitons,

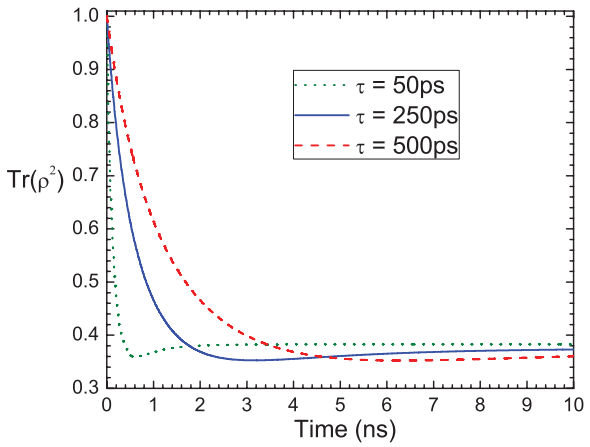

FIG. 8. (Color online) Trace of ρ^2 as a function of time with excitonic initial state and different coherence times.

the radiative lifetime is reported to be 290 ps,[43] while the dephasing of the excitonic spin may be taken as 30 ps, but can be drastically increased by the application of a static magnetic field.[44] Photon leakage can be estimated from Q factors; assuming a conservative value of $Q \simeq 5000$ yields a $\tau_{\rm ph} = 2Q/\omega \simeq 5$ ps; it is worth mentioning that cavities built from other materials can reach values of $Q = 160\,000$.[15,40] The decoherence time of Mn spins is larger or of the order of 10 μs.[45] Because photon leakage is the predominant decoherence channel, it was added to our model.

More precisely, we want to use the indirect interaction between Mn spins sitting in different QDs to realize two-qubit operations. Quantum computing with qubits larger than 1/2 is demonstrated by Bertaina *et al.*,[38] where a pair of states, for instance, $Sz = \pm 5/2$, can be chosen and the transitions between them controlled.

There are different ways to produce two-qubit operations; we have in mind the following sequence of operations on single spins plus an Ising interaction, that realizes a CNOT gate: $R^a_y(-\pi/2) \times R^b_z(-\pi/2) \times R^a_z(-\pi/2) \times U \times R^a_y(\pi/2)$, where $R^i_j(\theta)$ is a rotation of θ around the j axis of the qubit i.[25] From it, it is clear that an evolution operator $U = \exp(i\pi S^a_z S^b_z)$ can be written once an Ising Hamiltonian is given. In the absence of decoherence, it was shown that such Hamiltonian can be deduced from the more general one after tracing out the auxiliary excitons and photons degrees of freedom.[26] In the presence of decoherence, the reduction of the system plus bath to system still retaining information of the bath, hinders in general the construction of a Hamiltonian, and thus the ideal construction of the CNOT given above. However, as explained in previous sections, we can determine the effective parameters from the dynamics of the reduced density matrix. In any case, the presence of errors in the procedure yielding the Hamiltonian parameters propagates into the error of the CNOT gate.

From experimental studies, we take the values of the coupling constants as $J = 0.11$ meV, $g < 0.5$ meV.[46–49] Our calculation of Sec. III shows that the coupling can be as large as $I = 8\ \mu$eV, that will require an operation time of $\tau_I = 20.8$ ps. Also, we showed that the effective Hamiltonian can be found in the case of a photonic and an excitonic initial state, despite the fact that the former introduces more uncertainty in the Hamiltonian and thus the gate. We understand this difference in terms of antisymmetric (dark) states as explained in Ref. 50 and in Sec. III.

One observes that, for the time required to perform the operation τ_I, the purity of the state does not deviate substantially from 1 when the photon lifetime is above 250 ps (see insets of Figs. 4 and 8). This indicates that the state is only slightly nonpure. This ensures that we can approximately represent the problem using an effective Hamiltonian.

V. SUMMARY AND DISCUSSION

We have studied the dynamics of a system consisting of two quantum-dot excitons, each of which interacts with a localized spin, and strongly interacts with the main mode of a microcavity. This generates an effective Ising interaction I between the spins. We have included a finite lifetime of the cavity mode due to the leaking of the mode out of the cavity, which at present is the main source of decoherence in a number of systems with technological relevance. However, the extension to other sources of decoherence is trivial within our formalism and the results can be inferred from the present ones. The inclusion of decoherence effects seems essential to describe systems that can be assembled at present.

To extract I from the dynamics of the system, we have followed the time evolution of the reduced spin density matrix $\rho_{\rm eff}$ obtained after tracing out the photon and exciton degrees of freedom, for two different initial states which differed in the spin configuration.

An alternative procedure is the use of a stochastic Schrödinger equation (SSE),[51] in which the dynamics consists of a series of quantum trajectories, each composed by a non-Hermitian Hamiltonian evolution in between random sudden jumps. As expected from a non-Hermitian Hamiltonian, the probability is not conserved, and even in between jumps, the operator $U = \exp(-iH)$ will contain decay.[50] Because of this and the need to introduce quantum jumps, the SSE procedure does not provide a satisfactory solution to our present problem. Thus we have adopted the more practical procedure explained in Secs. II and III. From our analysis it becomes clear that, even at moderate photon decay times, we are able to resolve peaks that can be matched with certainty to those corresponding to the ideal case (no decoherence), allowing us to extract the parameters of a (quasi)effective Hamiltonian. We showed that there is an uncertainty on these parameters, which can be quantified from the width of the peaks. The broadening of the energy peaks points to decay, and so we obtain a result that qualitatively agrees with that of SSE. For the case of strong photon decay, adjacent peaks merge and the preceding analysis becomes unfeasible.

Instead of following the evolution of $\rho_{\rm eff}(t)$ for two different linear combinations of two eigenstates of $H_{\rm eff}$, another possibility is to choose one single linear combination of three eigenstates of $H_{\rm eff}$ and Fourier transform different off-diagonal elements of $\rho_{\rm eff}(t)$. This saves time but the price to pay is a smaller amplitude of the relevant peaks and therefore a larger error in the parameters of $H_{\rm eff}$.

For simplicity we have assumed a symmetric system and spin 5/2 as for Mn ions. The extension of the results when the excitonic energy E_x and the couplings g and J depend on i, and for arbitrary spin (in particular the effective spin ± 1 of Mn acceptors in II-V systems),[10] is straightforward. Our predictions for the parameters of the effective Hamiltonian might be tested using time-resolved Kerr rotation.[11]

Possible applications of the system were discussed in the previous section. At present it seems that the highest possible values of the cavity quality factor Q, or higher values of the Mn-exciton interaction J are needed to have a two-qubit operation not sensibly affected by the photon decoherence.

ACKNOWLEDGMENTS

We thank CONICET from Argentina for financial support. This work was partially supported by PIP 11220080101821 of CONICET, and PICT R1776 and PICT873/2007 of the ANPCyT.

[1] T. Pellizzari, S. A. Gardiner, J. I. Cirac, and P. Zoller, Phys. Rev. Lett. **75**, 3788 (1995).

[2] A. Imamoglu, D. D. Awschalom, G. Burkard, D. P. DiVincenzo, D. Loss, M. Sherwin, and A. Small, Phys. Rev. Lett. **83**, 4204 (1999).

[3] T. Calarco, A. Datta, P. Fedichev, E. Pazy, and P. Zoller, Phys. Rev. A **68**, 012310 (2003).

[4] G. F. Quinteiro, J. Fernandez-Rossier, and C. Piermarocchi, Phys. Rev. Lett. **97**, 097401 (2006).

[5] C. Bonato, F. Haupt, S. S. R. Oemrawsingh, J. Gudat, D. Ding, M. P. van Exter, and D. Bouwmeester, Phys. Rev. Lett. **104**, 160503 (2010).

[6] C. Le Gall, L. Besombes, H. Boukari, R. Kolodka, J. Cibert, and H. Mariette, Phys. Rev. Lett. **102**, 127402 (2009).

[7] D. E. Reiter, T. Kuhn, and V. M. Axt, Phys. Rev. Lett. **102**, 177403 (2009).

[8] M. Goryca, T. Kazimierczuk, M. Nawrocki, A. Golnik, J. A. Gaj, P. Kossacki, P. Wojnar, and G. Karczewski, Phys. Rev. Lett. **103**, 087401 (2009).

[9] A. H. Trojnar, M. Korkusiński, E. S. Kadantsev, P. Hawrylak, M. Goryca, T. Kazimierczuk, P. Kossacki, P. Wojnar, and M. Potemski, Phys. Rev. Lett. **107**, 207403 (2011).

[10] E. Baudin, E. Benjamin, A. Lemaître, and O. Krebs, Phys. Rev. Lett. **107**, 197402 (2011).

[11] A. Brunetti, M. Vladimirova, D. Scalbert, R. André, D. Solnyshkov, G. Malpuech, I. A. Shelykh, and A. V. Kavokin, Phys. Rev. B **73**, 205337 (2006).

[12] P. A. Dalgarno, M. Ediger, B. D. Gerardot, J. M. Smith, S. Seidl, M. Kroner, K. Karrai, P. M. Petroff, A. O. Govorov, and R. J. Warburton, Phys. Rev. Lett. **100**, 176801 (2008).

[13] L. M. León Hilario and A. A. Aligia, Phys. Rev. Lett. **103**, 156802 (2009).

[14] H. E. Türeci, M. Hanl, M. Claassen, A. Weichselbaum, T. Hecht, B. Braunecker, A. Govorov, L. Glazman, A. Imamoglu, and J. von Delft, Phys. Rev. Lett. **106**, 107402 (2011).

[15] J. P. Reithmaier, G. Seik, A. Loffler, C. Hofmann, S. Kuhn, S. Reitzenstein, L. V. Keldysh, V. D. Kulakovskii, T. L. Reinecke, and A. Forchel, Nature (London) **432**, 197 (2004).

[16] T. Yoshie, A. Scherer, J. Hendrickson, G. Khitrova, H. M. Gibbs, G. Rupper, C. Ell, O. B. Shchekin, and D. G. Deppe, Nature (London) **432**, 200 (2004).

[17] F. P. Laussy, E. del Valle, and C. Tejedor, Phys. Rev. B **79**, 235325 (2009).

[18] E. del Valle, F. P. Laussy, and C. Tejedor, Phys. Rev. B **79**, 235326 (2009).

[19] L. M. León Hilario, A. Bruchhausen, A. M. Lobos, and A. A. Aligia, J. Phys.: Condens. Matter **19**, 176210 (2007).

[20] A. Bruchhausen, L. M. León Hilario, A. A. Aligia, A. M. Lobos, A. Fainstein, B. Jusserand, and R. André, Phys. Rev. B **78**, 125326 (2008).

[21] T. Niemczyk, F. Deppe, H. Huebl, E. P. Menzel, F. Hocke, M. J. Schwarz, J. J. Garcia-Ripoll, D. Zueco, T. Hmmer, E. Solano, A. Marx, and R. Gross, Nat. Phys. **6**, 772 (2010).

[22] J. Casanova, G. Romero, I. Lizuain, J. J. García-Ripoll, and E. Solano, Phys. Rev. Lett. **105**, 263603 (2010).

[23] D. Braak, Phys. Rev. Lett. **107**, 100401 (2011).

[24] G. F. Quinteiro, Phys. Rev. B **77**, 075301 (2008).

[25] N. A. Gershenfeld and I. L. Chuang, Science **275**, 350 (1997).

[26] J. A. Andrade, A. A. Aligia, and G. F. Quinteiro, J. Phys.: Condens. Matter **23**, 215304 (2011).

[27] A. A. Aligia and T. Kroll, Phys. Rev. B **81**, 195113 (2010), and references therein.

[28] R. Raimondi, J. H. Jefferson, and L. F. Feiner, Phys. Rev. B **53**, 8774 (1996), and references therein.

[29] M. E. Simón, A. A. Aligia, and E. R. Gagliano, Phys. Rev. B **56**, 5637 (1997), and references therein.

[30] C. D. Batista and A. A. Aligia, Phys. Rev. B **47**, 8929 (1993).

[31] J. Bała, A. M. Oleś, and J. Zaanen, Phys. Rev. Lett. **72**, 2600 (1994).

[32] C. D. Batista, A. A. Aligia, and J. Eroles, Europhys. Lett. **43**, 71 (1998).

[33] P. Horsch, A. M. Oleś, L. F. Feiner, and G. Khaliullin, Phys. Rev. Lett. **100**, 167205 (2008), and references therein.

[34] C. Kittel, *Quantum Theory of Solids* (John Wiley and Sons, New York, 1963), p. 148.

[35] P. Meystre and M. Sargent, *Elements of Quantum Optics* (Springer, Berlin, 2007).

[36] A. Mitra and R. Vyas, Phys. Rev. A **81**, 012329 (2010).

[37] A. O. Govorov and A. V. Kalameitsev, Phys. Rev. B **71**, 035338 (2005).

[38] S. Bertaina, L. Chen, N. Groll, J. Van Tol, N. S. Dalal, and I. Chiorescu, Phys. Rev. Lett. **102**, 050501 (2009).

[39] W. Press, S. Teukolsky, W. Vetterling, and B. Flannery, *Numerical Recipes in C* (Cambridge University Press, New York, 1992), p. 507.

[40] S. Reitzenstein and A. Forchel, J. Phys. D **43**, 033001 (2010).

[41] T. Jakubczyk, T. Kazimierczuk, A. Golnik, P. Bienias, W. Pacuski, C. Kruse, D. Hommel, L. Kopotowski, T. Wojtowicz, and J. A. Gaj, Acta Phys. Pol. A **116**, 888 (2009).

[42] W.-M. Schulz, T. Thomay, M. Eichfelder, M. Bommer, M. Wiesner, R. Robach, M. Jetter, R. Bratschitsch, A. Leitenstorfer, and P. Michler, Opt. Express **18**, 12543 (2010).

[43] J. Suffczynski, T. Kazimierczuk, M. Goryca, B. Piechal, A. Trajnerowicz, K. Kowalik, P. Kossacki, A. Golnik, K. P. Korona, M. Nawrocki, J. A. Gaj, and G. Karczewski, Phys. Rev. B **74**, 085319 (2006).

[44] S. Mackowski, T. A. Nguyen, T. Gurung, K. Hewaparakrama, H. E. Jackson, L. M. Smith, J. Wrobel, K. Fronc, J. Kossut, and G. Karczewski, Phys. Rev. B **70**, 245312 (2004); Y. Chen, T. Okuno, Y. Masumoto, Y. Terai, S. Kuroda, and K. Takita, *ibid*. **71**, 033314 (2005).

[45] M. Goryca, D. Ferrand, P. Kossacki, M. Nawrocki, W. Pacuski, W. Maslana, J. A. Gaj, S. Tatarenko, J. Cibert, T. Wojtowicz, and G. Karczewski, Phys. Rev. Lett. **102**, 046408 (2009).

[46] G. Chiappe, J. Fernández-Rossier, E. Louis, and E. V. Anda, Phys. Rev. B **72**, 245311 (2005).

[47] L. Besombes, Y. Léger, L. Maingault, D. Ferrand, H. Mariette, and J. Cibert, Phys. Rev. Lett. **93**, 207403 (2004).

[48] Y. Léger, L. Besombes, J. Fernández-Rossier, L. Maingault, and H. Mariette, Phys. Rev. Lett. **97**, 107401 (2006).

[49] A. O. Govorov and A. V. Kalameitsev, Phys. Rev. B **71**, 035338 (2005).

[50] P. M. Visser and G. Nienhuis, Phys. Rev. A **52**, 4727 (1995).

[51] C. W. Gardiner and P. Zoller, *Quantum Noise*, 3rd ed. (Springer, Berlin, 2004).